Am J Cancer Res 2023;13(6):2360-2375
www.ajcr.us /ISSN:2156-6976/ajcr0147788

Original Article

Circular RNA hsa_circ_001350 contributes to osteosarcoma progression by regulating microRNA-578/CCR4-NOT transcription complex and subunit 7/Wnt signaling

Rujin Xu, Xingyuan Ci, Fang He, Yueqin Chen

Laboratory Department, Hangzhou Linping First People's Hospital, Hangzhou 311400, Zhejiang, P. R. China

Received November 16, 2022; Accepted April 24, 2023; Epub June 15, 2023; Published June 30, 2023

Abstract: Accumulating evidence has revealed that circular RNAs (circRNAs) play important roles in cancer by sponging microRNAs (miRNAs). A previous study has shown that hsa_circ_001350 expression is increased in glioma tissue samples and cells and that hsa_circ_001350 directly sponges miR-1236. Here, we investigated the role of hsa_circ_001350 in osteosarcoma (OS). Bioinformatics analysis was performed to examine the potential interactions among hsa_circ_001350, miR-578, and the CCR4-NOT transcription complex and subunit 7 (CNOT7). Reverse transcription-quantitative polymerase chain reaction and western blotting were performed to analyze gene expression and protein levels, respectively. Hsa_circ_001350 expression was upregulated in OS tissues and cell lines. The deletion of hsa_circ_001350 inhibited the proliferation, migration, and invasion of OS cells. The downregulation of hsa_circ_001350 suppressed CNOT7 expression by sponging miR-578 as confirmed by rescue experiments and luciferase reporter assays. Specifically, the depletion of hsa_circ_001350 inhibited the protein expression of β-catenin, cyclin D1, and c-myc in OS cells, and CNOT7 overexpression reversed this effect. We conclude that hsa_circ_001350 contributes to OS progression by regulating miR-578/CNOT7/Wnt signaling. Thus, hsa_circ_001350, miR-578, and CNOT7 may be potential targets for the treatment of OS.

Keywords: Osteosarcoma, hsa_circ_001350, miR-578, CNOT7, Wnt signaling

Introduction

Osteosarcoma (OS) is a prevalent bone malignancy originating from mesenchymal cells and has a high mortality rate in adolescents and children [1, 2]. Improved operational methods combined with various chemotherapies have been applied clinically; however, the incidence remains unchanged, and numerous patients experience recurrence because of potential or existing remote metastases [3, 4]. Additional therapies, such as small molecule targeted drugs, may benefit patients with OS patients; however, these treatments usually result in severe side effects and are clinically ineffective [5]. Consequently, exploring the complicated OS regulatory axis is urgently required to develop more practical therapeutic strategies.

Circular RNAs (circRNAs) are an emerging type of non-coding RNA that play a critical role in the progression of various cancers [6, 7]. Hsa_circ_001350 also known as hsa_circ_0000253 or circBLNK, is located on chr10:97999787 to 97999925, which belongs to the human BLNK locus [8]. Hsa_circ_001350 contributes to tumorigenesis in glioma [8]. Circ_0000253 promotes OS progression via the miR-1236-3p/SP1 axis [9]. Recent studies have shown that circRNAs function as "sponges" for microRNAs (miRNAs), blocking the inhibitory effect of miRNAs on downstream target gene expression [10, 11]. Circ_001621 contributes to the migration and proliferation of OS cells by sponging miR-578, causing unregulated VEGF expression [12]. However, the regulatory mechanisms of miR-578 in OS remain unclear.

In addition, CCR4-NOT transcription complex and subunit 7 (CNOT7) has been identified as an oncogene in several cancers, including hepatocellular carcinoma and breast cancer

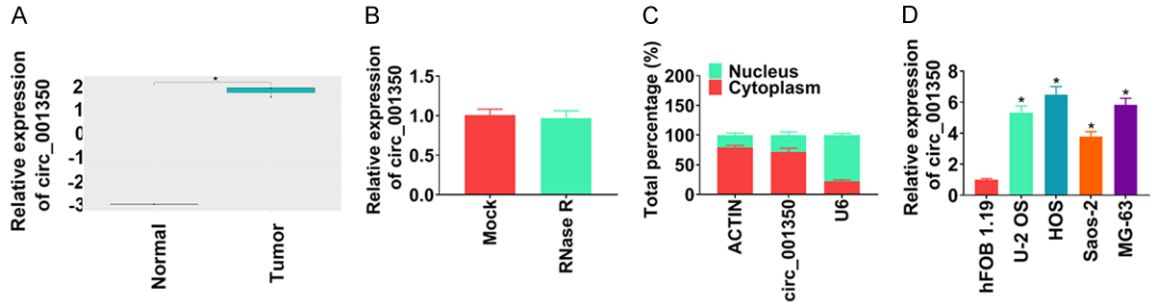

Figure 1. Hsa_circ_001350 is highly expressed in clinical osteosarcoma (OS) samples and OS cells. A. The expression of hsa_circ_001350 was analyzed in the adjacent tissues and tumor tissues of 3 patients obtained from GSE140256. B. Total RNA was digested with RNase R, and then hsa_circ_001350 was examined by RT-qPCR. C. Subcellular localization of hsa_circ_001350 was examined by RT-qPCR after nuclear-cytoplasm fractionation. D. The expression of hsa_circ_001350 was measured by RT-qPCR in hFOB 1.19, U-2OS, HOS, Saos-2, and MG-63 cells. N = 3, mean ± SD, $^*P < 0.05$.

[13, 14]. The Wnt signaling pathway regulates cell proliferation and differentiation [15]. Circ_001569 expression is upregulated in OS, and it promotes cell proliferation and cisplatin resistance by activating the Wnt/β-catenin signaling pathway [16]. However, whether miR-578, CNOT7, and the Wnt signaling pathway are involved in hsa_circ_001350-mediated OS progression remains unclear.

In this study, we explored the effects of hsa_circ_001350 on OS development and the underlying mechanisms. We found that hsa_circ_001350 enhanced the development of OS via miR-578/CNOT7/Wnt signaling.

Materials and methods

Cell culture and treatment

Normal human osteoblasts hFOB 1.19, OS U-2OS, HOS, Saos-2, and MG-63 cell lines (Procell, Wuhan, China) were maintained in the laboratory. The cells were cultured in an incubator at 5% CO_2 and 37°C in Dulbecco's Modified Eagle Medium containing fetal bovine serum (FBS; 10%, GE, USA), streptomycin (0.1 mg/mL, GE, USA), and penicillin (100 units/mL, GE, USA). Hsa_circ_001350 small interfering RNA (siRNA) and si-negative control (NC) were obtained from Tsingke Biotechnology Co., Ltd. (Beijing, China), and the pcDNA3.1-CNOT7 overexpression vector, pcDNA3.1-NC, miR-578 mimic, mimic NC, miR-578 inhibitor, and inhibitor NC were obtained from GenePharma (Shanghai, China). The cells (5×10^5 cells/well) were seeded in 6-well plates. The cells were transfected using Lipofectamine 3000 (Invitrogen, USA) at 37°C for 6 h. The following concentrations were used for transfection: siNC, 50 nM; si-hsa_circ_001350, 50 nM; pcDNA3.1-NC, 50 nM; pcDNA3.1-CNOT7, 50 nM; miR-578 mimics, 45 nM; mimic NC, 45 nM; miR-578 inhibitor, 45 nM; and inhibitor NC, 45 nM. After transfection for 48 h at 37°C, the cells were collected for subsequent experiments. The sequences used were as follows: hsa_circ_001350: si-1 sense: 5'-CAAGAAAGCAAACAGGUAAAU-3', antisense: 5'-UUACCUGUUUGCUUUCUUGUU-3', si-2 sense: 5'-AGCAAACAGGUAAAUAUAAAU-3', antisense: 5'-UUAUAUUUACCUGUUUGCUUU-3', si-NC sense: 5'-UUCUCCGAACGUGUCACGUTT-3', antisense: 5'-ACGUGACACGUUCGGAGAATT-3', hsa-miR-578 mimic sense: 5'-CUUCUUGUGCUCUAGGAUUGU-3', hsa-miR-578 mimic antisense: 5'-AAUCCUAGAGCACAAGAAGUU-3', mimic NC sense: 5'-UUCUCCGAACGUGUCACGUTT-3', mimic NC antisense: 5'-ACGUGACACGUUCGGAGAATT-3', hsa-miR-578 inhibitor: 5'-ACAAUCCUAGAGCACAAGAAG-3', inhibitor NC: 5'-CAGUACUUUUGUGUAGUACAA-3'. For western blotting, the cells were treated with 20 mM LiCl (cat. No. L9650; Sigma-Aldrich, USA) for 3 h at 37°C.

EdU assays

Cell proliferation was analyzed by an EdU assay using an EdU detection kit (RiboBio, China). Briefly, the transfected cells were grown in 24-well plates (2×10^4 cells/well) and cultured with EdU at 37°C for 2 h. The cells were fixed in 4% paraformaldehyde at room temperature for

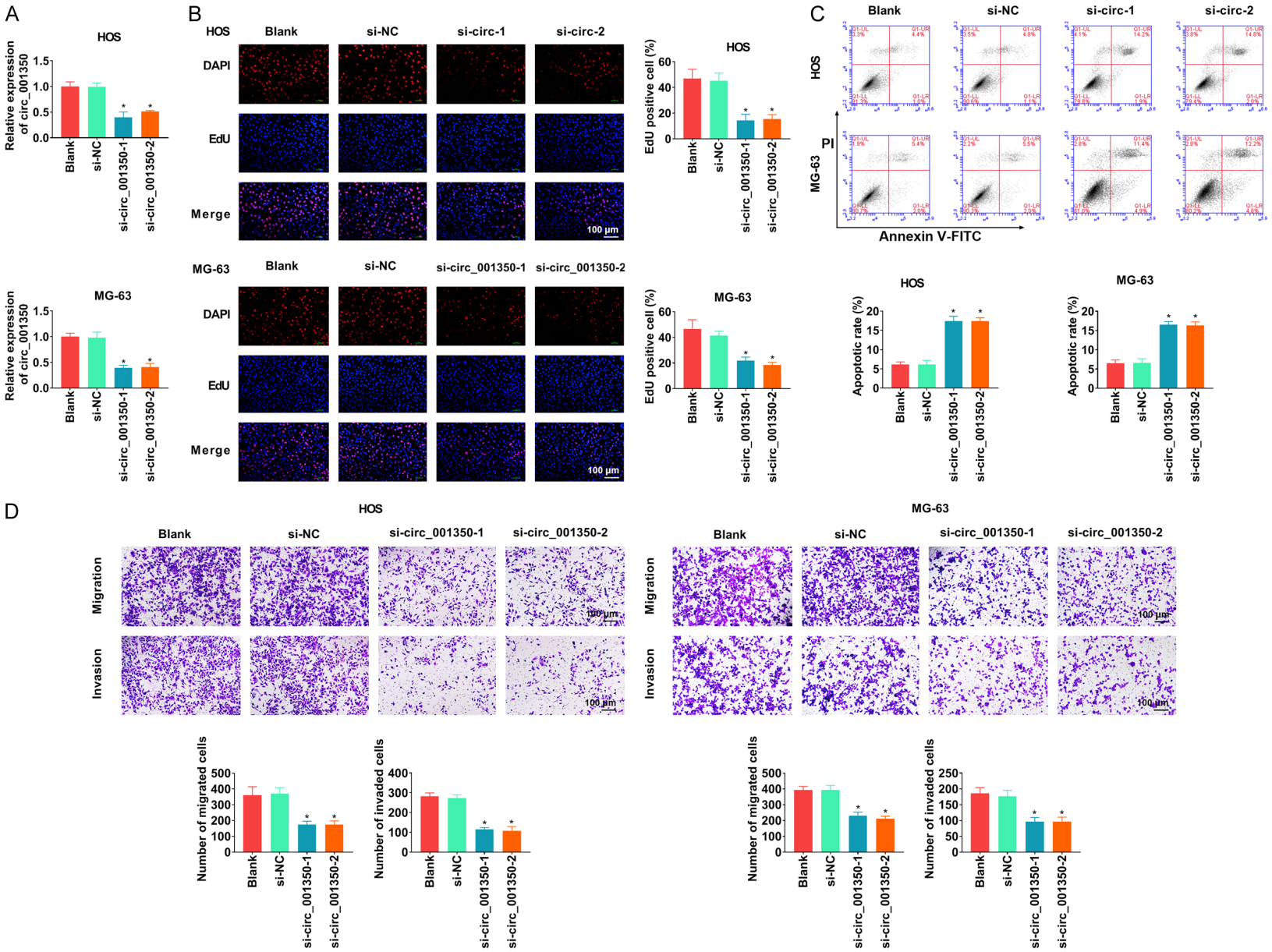
A
HOS
Relative expression of circ_001350
Blank
si-NC
si-circ_001350-1
si-circ_001350-2
MG-63
B
HOS
Blank
si-NC
si-circ-1
si-circ-2
DAPI
EdU
Merge
100 μm
EdU positive cell (%)
MG-63
si-circ_001350-1
si-circ_001350-2
C
Blank
si-NC
si-circ-1
si-circ-2
HOS
MG-63
PI
Annexin V-FITC
Apoptotic rate (%)
D
Migration
Invasion
Number of migrated cells
Number of invaded cells

Figure 2. Hsa_circ_001350 effects proliferation, migration, and invasion of OS cells. A. HOS and MG-63 cells were transfected with hsa_circ_001350 siRNA-1 or hsa_circ_001350 siRNA-2. The expression of hsa_circ_001350 was measured by RT-qPCR. B. The cell proliferation was analyzed by EdU assay. C. Apoptosis was detected by flow cytometry. D. The migration and invasion were tested by transwell assays in the cells. N = 3, mean ± SD, $^{*}P < 0.05$.

30 min. The cells were then permeabilized with Triton X-100 (0.4%, 10 min) and stained with an EdU staining cocktail in the dark (room temperature, 30 min). The nuclei of the cells were stained with DAPI (room temperature, 30 min). Images of five randomly selected areas in each group were captured using a fluorescence microscope (Eclipse Ti2-U; Nikon Corporation; magnification, 400 ×). EdU-positive cells were quantified using the ImageJ software (Version: V1.8.0.112, National Institutes of Health).

Apoptosis

According to the manufacturing instructions of Annexin V-FITC/PI Apoptosis Detection Kit (Vazyme), the apoptosis rate in HOS and MG-63 cells was detected. Briefly, the cells were washed in phosphate-buffered saline and suspended in the Annexin V binding buffer. Annexin V-fluorescein isothiocyanate and propidium iodide were added to the cells for 15 min. The rate of apoptosis was determined by flow cytometry.

Western blot analysis

Radioimmunoprecipitation assay buffer (CST, USA) was used to extract the total protein, which was quantified using the bicinchoninic acid method (Abbkine, USA). The protein (30 μg) was subjected to sodium dodecyl sulfate-polyacrylamide gel electrophoresis and transferred to polyvinylidene fluoride membranes (Millipore, USA), followed by incubation with 5% milk and primary antibodies at 4°C overnight. The membranes were incubated with the corresponding secondary antibodies (BOSTER, China) for 1 h at room temperature, followed by visualization using a chemiluminescence detection kit (Beyotime, China). The primary antibodies comprised CNOT7 (Abcam, USA), β-catenin (Abcam, USA), cyclin D1 (Abcam, USA), c-myc (Abcam, USA), and β-actin (Abcam, USA).

Transwell assays

Transwell assays were performed to analyze the invasion and migration of OS cells using Transwell plates (Corning, USA), according to the manufacturer's instructions. Briefly, the upper chambers were inoculated with approximately 1×10^5 cells, and a medium containing 10% FBS was added to the lower chambers. The cells were solidified using 4% paraformaldehyde (Beyotime Biotechnology Co., Shanghai, China) at room temperature for 10 min and stained with 0.5% crystal violet (Sigma-Aldrich, MO, USA) for 10 min. The numbers of invading and migrating cells were recorded and counted under an inverted microscope (Olympus, Tokyo, Japan). For the invasion assay, the upper chambers were pre-coated with diluted Matrigel (1:8, Qcbio Science and Technologies Co., Ltd., Shanghai, China).

Reverse transcription-quantitative polymerase chain reaction (RT-qPCR)

Total RNA was isolated using the TRIzol reagent (Solarbio, China). The purified RNA was treated with or without RNase R (Guangzhou Geneseed Biotech Co., Ltd.) to assess circRNA expression. The quality of total RNA was determined at a 260/280 nm absorbance ratio using a NanoDrop Life spectrophotometer (Thermo Fisher Scientific). RNA (1 μg) was reverse-transcribed using the PrimeScript™ 1st Strand cDNA Synthesis Kit (TaKaRa, China). The qPCR was performed using SYBR-Green (Takara, China). For miR-578 expression, a total of 1 μg miRNA was reverse transcripted using miRNA 1st Strand cDNA Synthesis Kit (by stem-loop) (Vazyme, Nanjing, China) and miR-578 expression was detected using miRNA Universal SYBR qPCR Master Mix (Vazyme, Nanjing, China). The primer sequences used were as follows: hsa_circ_001350: 5'-GGGGAATCAGTGTGGGGTAG-3', 5'-ACAGCAGGTACCATGTTTGCTA-3'; miR-578: 5'-GCGGCGGCTTCTTGTGCTCTAG-3', 5'-ATCCAGTGCAGGGTCCGAGG-3'; GAPDH: 5'-CATGTTGCAACCGGGAAGGA-3', 5'-GCCCAATACGACCAAATCAGAG-3'; U6: 5'-CAGCACATATACTAAAATTGGAACG-3', 5'-ACGAATTTGCGTGTCATCC-3'.

Nuclear and cytoplasmic fractions

The PARIS™ kit (Invitrogen, USA) was used to determine the location of hsa_circ_001350.

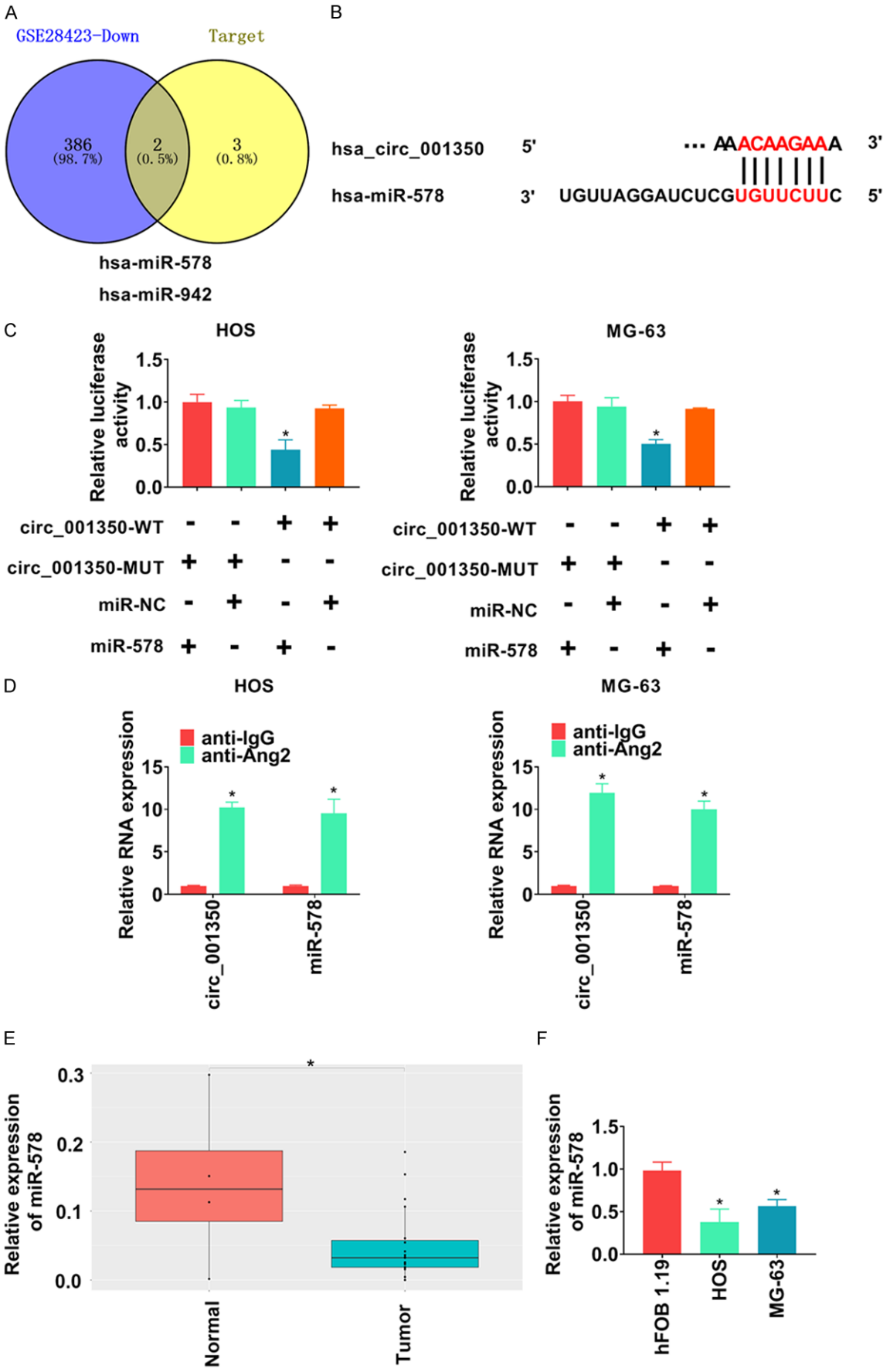
A
GSE28423-Down
Target
386
(98.7%)
2
(0.5%)
3
(0.8%)
hsa-miR-578
hsa-miR-942
B
hsa_circ_001350 5' ··· AAACAAGAAA 3'
hsa-miR-578 3' UGUUAGGAUCUCGUGUUCUUC 5'
C
HOS
MG-63
Relative luciferase activity
circ_001350-WT
circ_001350-MUT
miR-NC
miR-578
D
HOS
MG-63
anti-IgG
anti-Ang2
Relative RNA expression
circ_001350
miR-578
E
Relative expression of miR-578
Normal
Tumor
F
Relative expression of miR-578
hFOB 1.19
HOS
MG-63

Figure 3. Hsa_circ_001350 serves as a sponge of miR-578 in OS cells. A. The abnormally expressed miRNAs were analyzed in samples from GSE28423. The potential interacted miRNAs of hsa_circ_001350 was analyzed in the bioinformatics analysis. Overlap analysis was performed based on these two analyses. B. The potential interaction between miR-578 and hsa_circ_001350 was identified in the bioinformatics analysis. C. HOS and MG-63 cells were transfected with the miR-578 mimic or control mimic, or co-treated with miR-578 mimic and pmirGLO-hsa_circ_001350 or pmirGLO-hsa_circ_001350 mutant. The luciferase activity was determined by luciferase reporter assay. D. The RIP assay was conducted in HOS and MG-63 cells using Anti-Ago2 to investigate the relationship between circ_001350 and miR-578 and Anti-IgG was used as the control. E. The expression of miR-578 was analyzed in 19 OS cell lines and 4 normal bones obtained from GSE28423. F. The expression of miR-578 was measured by RT-qPCR in hFOB 1.19, U-2OS, HOS, and MG-63 cells. N = 3, mean ± SD, $^{*}P < 0.05$ vs. circ_001350-WT+miR-NC, normal, or hFOB 1.19 group.

The expression of hsa_circ_001350 in the nuclear and cytoplasmic fractions was determined by RT-qPCR. The efficiency of nuclear and cytoplasmic RNA isolation was controlled by U6 and actin, respectively.

Luciferase reporter gene assay

Luciferase reporter gene assays were performed using Dual-Luciferase Reporter Assay System (Promega, USA). The cells were transfected with pmirGLO-hsa_circ_001350 or pmirGLO-CNOT7, and miR-578 mimic or control mimic using riboFECT™ CP Transfection Kit (RiboBio, China). Luciferase activity was then analyzed. *Renilla* luciferase activity was measured as a control.

RNA immunoprecipitation (RIP) assay

RIP was performed using Magna RIP RNA-Binding Protein Immunoprecipitation Kit (Millipore, Bedford, MA, USA) following the manufacturer's protocol. Briefly, cultured HOS and MG-63 cells were lysed in the RIP lysis buffer (Solarbio), and the cell extracts were incubated with magnetic beads conjugated with the human anti-AGO2 antibody (Millipore) and control IgG (Merck Millipore) for 8 h at 37°C. Subsequently, the magnetic beads were incubated with proteinase K. Immunoprecipitated RNA was analyzed by RT-qPCR.

Bioinformatics analysis

Samples were obtained from the Gene Expression Omnibus (GEO) database (GSE140256, GSE28423, and GSE42572). Potential interactions of miR-578 with hsa_circ_001350 and CNOT7 were analyzed using CircInteractome (https://circinteractome.nia.nih.gov/), MIRDB (http://www.microrna.org/) and TargetScan (http://www.targetscan.org/vert_72/). Gene set enrichment analysis (GSEA) was performed using the GSEA software (http://software.broadinstitute.org/gsea/index.jsp). GSEA was performed using the GSE140256 dataset. The annotated gene set file (h.all.v7.0.entrez.gmt, http://www.gsea-msigdb.org/gsea/downloads.jsp) was used as a reference. The translational ability of circ_001350 was predicted using circBank (http://www.circbank.cn/searchCirc.html).

Statistical analysis

Data are presented as the mean ± standard deviation, and statistical analyses were performed using the SPSS software (version 18.0). Unpaired Student's *t*-test was used for comparisons between two groups, and one-way analysis of variance was used for comparisons among multiple groups. $P < 0.05$ was considered statistically significant.

Results

Hsa_circ_001350 is highly expressed in OS samples and cells

To explore the function of hsa_circ_001350 in OS progression, we analyzed its expression using the GEO database. We found that the expression of hsa_circ_001350 was significantly upregulated in the clinical samples obtained from the GSE140256 dataset (**Figure 1A**). The prediction results of circBANK showed that CIRC might not have translational ability (circRNA_size: 414, open reading frame_size: 87, Fickett_score: 0.5834, Hexamer_score: -0.1173, coding_prob: 0.0037). Hsa_circ_001350 was resistant to RNase R digestion (**Figure 1B**). As shown in **Figure 1C**, hsa_circ_001350 was primarily localized in the cytoplasm. The expression of hsa_circ_001350 was up-regulated in the OS cell lines, including

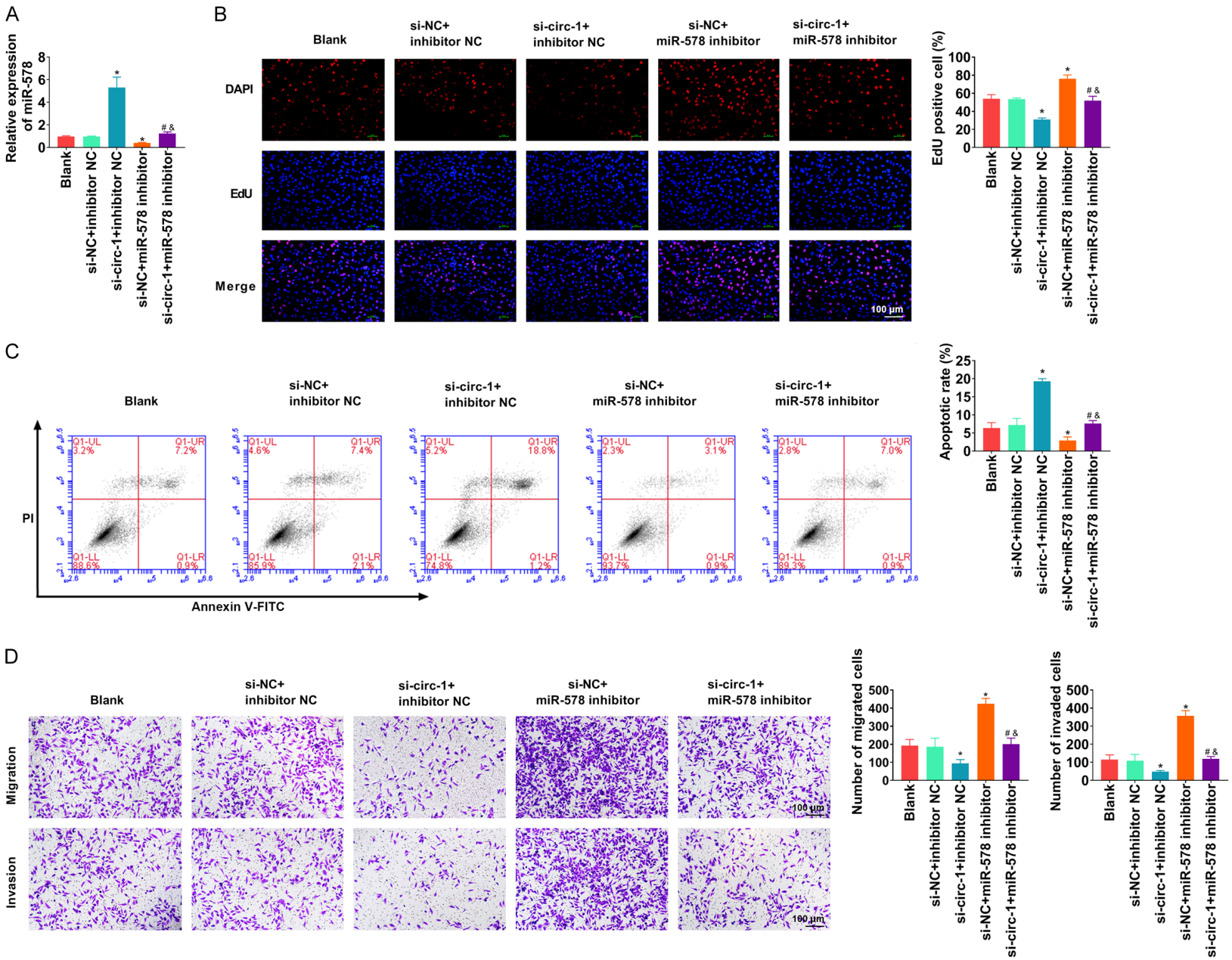
A
Relative expression of miR-578
Blank
si-NC+inhibitor NC
si-circ-1+inhibitor NC
si-NC+miR-578 inhibitor
si-circ-1+miR-578 inhibitor
B
Blank
si-NC+ inhibitor NC
si-circ-1+ inhibitor NC
si-NC+ miR-578 inhibitor
si-circ-1+ miR-578 inhibitor
DAPI
EdU
Merge
100 μm
EdU positive cell (%)
C
PI
Annexin V-FITC
Q1-UL 3.2%
Q1-UR 7.2%
Q1-LL 88.6%
Q1-LR 0.9%
Q1-UL 4.6%
Q1-UR 7.4%
Q1-LL 85.9%
Q1-LR 2.1%
Q1-UL 5.2%
Q1-UR 18.8%
Q1-LL 74.8%
Q1-LR 1.2%
Q1-UL 2.3%
Q1-UR 3.1%
Q1-LL 93.7%
Q1-LR 0.9%
Q1-UL 2.8%
Q1-UR 7.0%
Q1-LL 89.3%
Q1-LR 0.9%
Apoptotic rate (%)
D
Migration
Invasion
100 μm
Number of migrated cells
Number of invaded cells

Figure 4. Hsa_circ_001350 enhances proliferation, migration, and invasion of OS cells by targeting miR-578. A. The HOS cells were co-transfected with si-NC and inhibitor NC, hsa_circ_001350 siRNA-1 and inhibitor NC, si-NC and miR-578 inhibitor, hsa_circ_001350 siRNA-1 and miR-578 inhibitor. The expression of miR-578 was measured by RT-qPCR. B. The cell proliferation was assessed by EdU assays. C. Apoptosis was detected by flow cytometry. D. The migration and invasion were determined by transwell assays. N = 3, mean ± SD, $^{*}P < 0.05$ vs. si-NC+inhibitor NC group, $^{\#}P < 0.05$ vs. si-circ-1+inhibitor NC group, $^{\&}P < 0.05$ vs. si-NC+miR-578 inhibitor group.

U-2OS, HOS, Saos-2, and MG-63 cells, compared with that in normal osteoblast hFOB 1.19 cells (**Figure 1D**), implying that hsa_circ_001350 might be closely associated with OS progression.

Hsa_circ_001350 reduces proliferation, migration, and invasion

Given that the expression of hsa_circ_001350 was the highest in HOS and MG-63 cells, we selected these two cell lines for subsequent experiments. HOS and MG-63 cells were transfected with hsa_circ_001350 siRNA and the transfection efficiency was confirmed (**Figure 2A**). The EdU assays showed that the depletion of hsa_circ_001350 significantly reduced the proliferation of HOS and MG-63 cells (**Figure 2B**). Knockdown of hsa_circ_001350 induced apoptosis (**Figure 2C**). Moreover, the migration and invasion of HOS and MG-63 cells were markedlyrepressed by hsa_circ_001350 siRNA (**Figure 2D**), suggesting that hsa_circ_001350 depletion reduced the proliferation, migration, and invasion of OS cells.

Hsa_circ_001350 serves as a sponge of miR-578 in OS cells

To investigate the mechanism of hsa_circ_001350-mediated OS progression, miRNA expression was analysed in the OS cell line GSE28423, and potential miRNA interactions associated with hsa_circ_001350 were assessed via bioinformatics analysis. Overlap analysis identified miR-578 as a potential target of hsa_circ_001350 (**Figure 3A** and **3B**). MiR-578 mimic remarkably suppressed the luciferase activity of hsa_circ_001350 in HOS and MG-63 cells (**Figure 3C**). The RIP assay indicated that the relative enrichment of hsa_circ_001350 and miR-578 was higher in the Anti-Ago2 group than in the control group (**Figure 3D**). In addition, the expression of miR-578 was downregulated in the OS cell line from GSE28423 (**Figure 3E**). The expression of miR-578 was also down-regulated in HOS and MG-63 cells compared with that in normal osteoblast hFOB 1.19 cells (**Figure 3F**).

Hsa_circ_001350 enhances proliferation, migration, and invasion of OS cells by targeting miR-578

We observed that the depletion of hsa_circ_001350 enhanced miR-578 expression, whereas miR-578 inhibitor induced the opposite effect (**Figure 4A**). Furthermore, miR-578 inhibitor rescued EdU-positive HOS cells attenuated by hsa_circ_001350 siRNA (**Figure 4B**). MiR-578 inhibitor abrogated hsa_circ_001350 siRNA-induced apoptosis (**Figure 4C**). The depletion of hsa_circ_001350 reduced the migration and invasion of HOS cells, whereas the miR-578 inhibitor reversed this effect (**Figure 4D**), indicating that hsa_circ_001350 enhanced proliferation, migration, and invasion of OS cells by targeting miR-578.

MiR-578 targets CNOT7 in OS cells

Then, we performed an overlap analysis of the up-regulated genes in the clinical samples obtained from GSE42572 and potential interactions between mRNAs and miR-578 were identified via bioinformatics analysis. Interestingly, we found that CNOT7 expression was upregulated in the tumor samples compared with that in normal samples from GSE42572 and that CNOT7 had a binding site within the mRNA 3'UTR (**Figure 5A** and **5B**). We confirmed that miR-578 mimic reduced the luciferase activity of CNOT7 in HOS and MG-63 cells (**Figure 5C**). HOS and MG-63 cells were transfected with miR-578 mimic or inhibitor, and the transfection efficiency was verified (**Figure 5D**). The protein levels of CNOT7 in the cells were decreased by miR-578 mimic and increased by miR-578 inhibitor (**Figure 5E**). Furthermore, the expression of CNOT7 was upregulated in tumor samples compared with that in normal samples from GSE42572 (**Figure 5F**). CNOT7 expression was down-regulated in

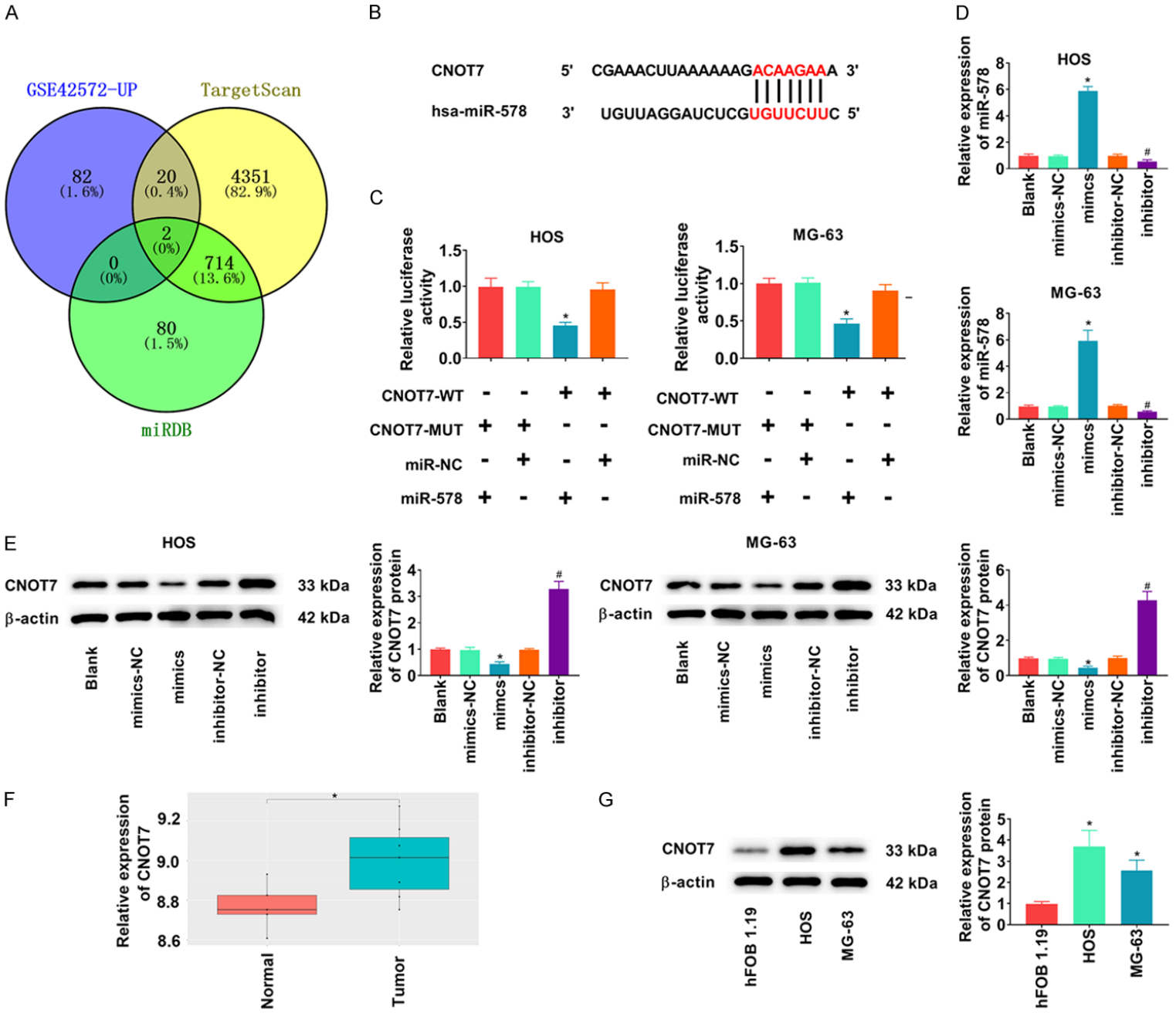
A
GSE42572-UP
TargetScan
miRDB
82
(1.6%)
20
(0.4%)
4351
(82.9%)
2
(0%)
0
(0%)
714
(13.6%)
80
(1.5%)
B
CNOT7 5' CGAAACUUAAAAAAGACAAGAAA 3'
hsa-miR-578 3' UGUUAGGAUCUCGUGUUCUUC 5'
C
HOS
MG-63
Relative luciferase activity
CNOT7-WT
CNOT7-MUT
miR-NC
miR-578
D
HOS
MG-63
Relative expression of miR-578
Blank
mimics-NC
mimcs
inhibitor-NC
inhibitor
E
HOS
MG-63
CNOT7
β-actin
33 kDa
42 kDa
Relative expression of CNOT7 protein
F
Relative expression of CNOT7
Normal
Tumor
G
hFOB 1.19
HOS
MG-63

Figure 5. MiR-578 targets CNOT7 in OS cells. A. The abnormally expressed mRNA was analyzed in samples obtained from GSE42572. The potential interacted mRNAs with miR-578 was analyzed in the bioinformatics analysis using MIRDB and TargetScan database. The overlap analysis was performed based on these two analyses. B. The potential interaction between miR-578 and CNOT7 was identified in the bioinformatics analysis. C. HOS and MG-63 cells were transfected with the miR-578 mimic or control mimic, or co-transfected with miR-578 mimic and pmirGLO-CNOT7 or pmirGLO-CNOT7 mutant. The luciferase activity was determined by luciferase reporter assay. D. HOS and MG-63 cells were transfected with the miR-578 mimic or inhibitor. The expression of miR-578 was validated by RT-qPCR. E. The protein expression of CNOT7 was measured by western blotting, followed by the quantification analysis using ImageJ. F. The expression of CNOT7 was examined in the clinical samples obtained from GSE42572. G. The expression of CNOT7 was tested by RT-qPCR in hFOB 1.19, U-2OS, HOS, and MG-63 cells. N = 3, mean ± SD, $^{*}P < 0.05$ vs. CNOT7-WT+miR-NC, mimics-NC, normal, or hFOB 1.19 group, $^{\#}P < 0.05$ vs. inhibitor-NC group.

HOS and MG-63 cells compared with that in hFOB 1.19 cells (**Figure 5G**).

Hsa_circ_001350 promotes the proliferation, migration, and invasion of OS cells by increasing CNOT7 protein levels

HOS cells were transfected with pcDNA3.1-CNOT7 and the transfection efficiency was confirmed (**Figure 6A**). Hsa_circ_001350 significantly decreased the protein levels of CNOT7 in HOS cells, whereas the reconstitution of CNOT7 reversed this effect (**Figure 6B**). As expected, CNOT7 overexpression enhanced the hsa_circ_001350 siRNA-mediated inhibition of EdU positive HOS cells (**Figure 6C**). CNOT7 overexpression decreased hsa_circ_001350 siRNA-induced apoptosis (**Figure 6D**). Hsa_circ_001350 depletion decreased the migration and invasion of HOS cells, whereas CNOT7 reconstitution reversed this effect (**Figure 6E**), indicating that hsa_circ_001350 promotes the proliferation, migration, and invasion of OS cells by increasing CNOT7 protein levels.

Hsa_circ_001350 contributes to the proliferation, migration, and invasion of OS cells by regulating CNOT7/Wnt signaling

GSEA indicated that enrichment of the Wnt signaling pathway was associated with an increase in CNOT7 (**Figure 7A**). The depletion of hsa_circ_001350 notably attenuated the protein expression of β-catenin, cyclin D1, and c-myc in HOS and MG-63 cells (**Figure 7B**). LiCl rescued β-catenin, cyclin D1, and c-myc expression, which was repressed by hsa_circ_001350 knockdown in HOS cells (**Figure 7C**). Importantly, CNOT7 overexpression also rescued β-catenin, cyclin D1, and c-myc expression, which was repressed by hsa_circ_001350 knockdown in HOS cells (**Figure 7D**).

Discussion

OS is the most prevalent bone cancer, with a high incidence and limited therapeutic options. CircRNAs have been identified as critical regulators of OS tumorigenesis; however, the effect of hsa_circ_001350 on OS development remains unclear. In the present study, we showed that hsa_circ_001350 enhanced the malignant progression of OS via miR-578/CNOT7/Wnt signaling.

Several studies have provided evidence for the function of circRNAs in the pathogenesis of OS [17, 18]. Has_ circ_001350 modulates metastatic properties, apoptosis, and proliferation of glioma cells by sponging miRNAs [8]. Circ_0000253 promotes OS progression via the miR-1236-3p/SP1 axis [9]. Our data showed consistent results, hsa_circ_001350 was highly expressed in clinical OS samples and OS cells. Hsa_circ_001350 knockdown reduces the proliferation, migration, and invasion of OS cells. These results indicate that hsa_circ_001350 functions as an oncogene in OS development and provide valuable evidence for the role of circRNAs in OS regulation.

MiR-578 is a tumor suppressor in many cancers. Hsa_circ_0008673 enhances breast cancer progression via miR-578/GINS4 axis [19]. Blocking circ-LARP1B suppresses tumorigenicity and promotes radiosensitivity by regulating miR-578/IGF1R axis in hepatocellular carcinoma [20]. In addition, circ-CNST knockdown restrains malignant behavior of OS cells and inhibits glycolysis via circ-CNST/miR-578/LDHA/PDK1 axis [21]. Our data revealed that hsa_circ_001350 served as a sponge for miR-578 in OS cells and that hsa_circ_001350 promoted the proliferation, migration, and invasion of OS cells by targeting miR-578, which was in accordance with previous study [12].

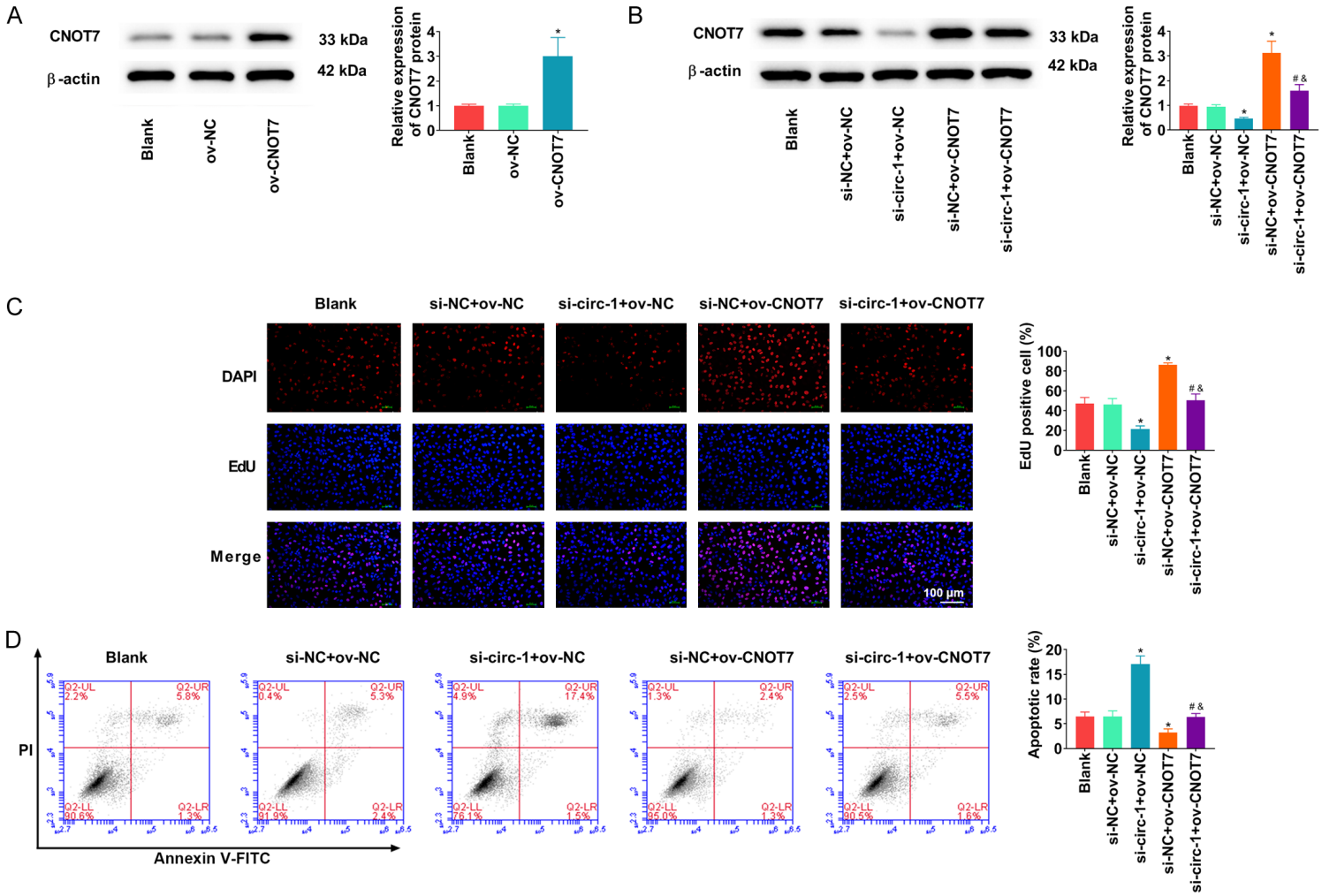
A
CNOT7
β-actin
33 kDa
42 kDa
Blank
ov-NC
ov-CNOT7
Relative expression of CNOT7 protein
B
si-NC+ov-NC
si-circ-1+ov-NC
si-NC+ov-CNOT7
si-circ-1+ov-CNOT7
C
DAPI
EdU
Merge
100 μm
EdU positive cell (%)
D
PI
Annexin V-FITC
Apoptotic rate (%)

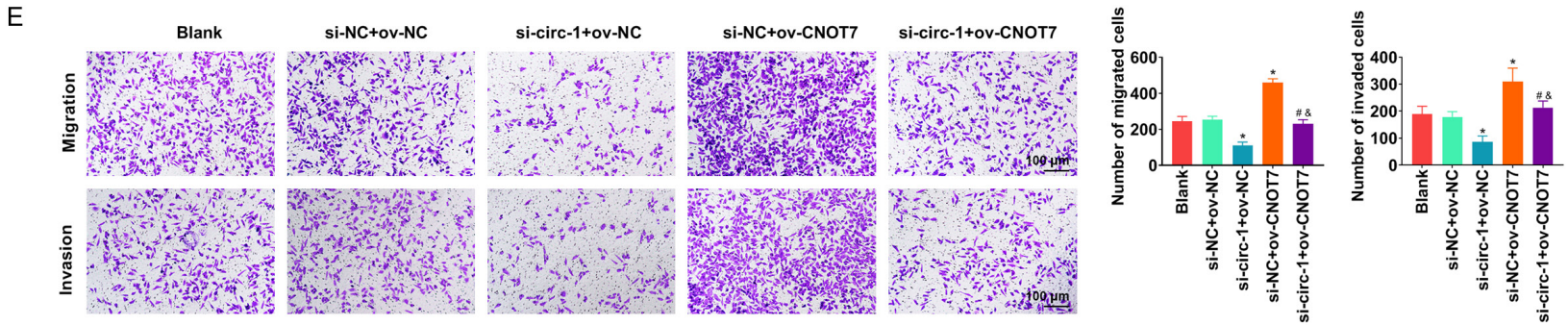

Figure 6. Hsa_circ_001350 promotes proliferation, migration, and invasion of OS cells by enhancing CNOT7. A. HOS cells were transfected with pcDNA3.1-NC or pcDNA3.1-CNOT7. The protein expression of CNOT7 was measured by western blotting in the cells, followed by the quantification analysis using ImageJ. B. The HOS cells were transfected with hsa_circ_001350 siRNA-1, or co-transfected with hsa_circ_001350 siRNA-1 and pcDNA3.1-CNOT7. The protein expression of CNOT7 was measured by western blotting in the cells, followed by the quantification analysis using ImageJ. C. The cell proliferation was analyzed by EdU assay. D. Apoptosis was detected by flow cytometry. E. The migration and invasion were assessed by transwell assay. N = 3, mean ± SD, $^{*}P < 0.05$ vs. si-NC+ov-NC group, $^{\#}P < 0.05$ vs. si-circ-1+ov-NC group, $^{\&}P < 0.05$ vs. si-NC+ov-CNOT7 group.

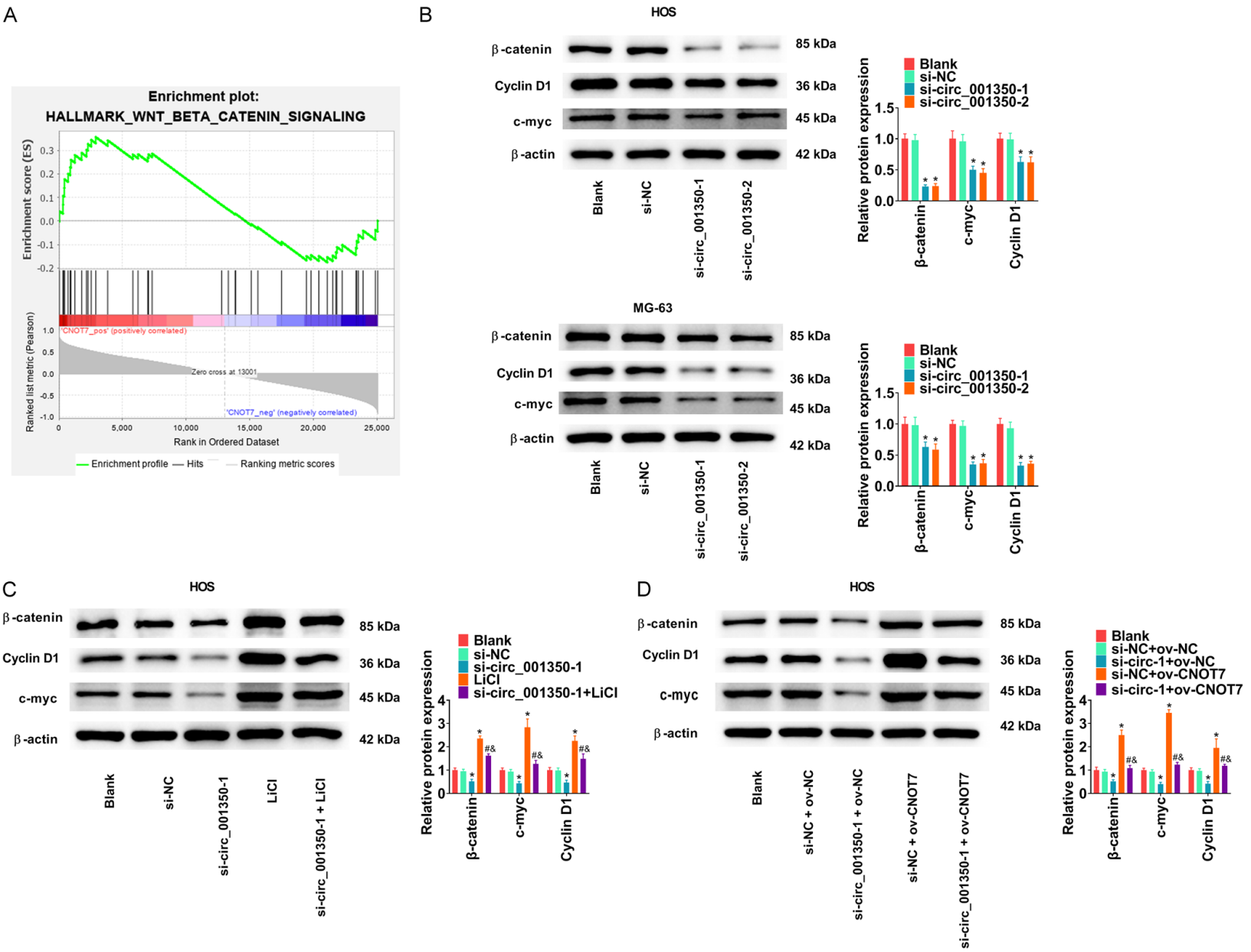
A
Enrichment plot:
HALLMARK_WNT_BETA_CATENIN_SIGNALING
Enrichment score (ES)
'CNOT7_pos' (positively correlated)
Zero cross at 13001
'CNOT7_neg' (negatively correlated)
Ranked list metric (Pearson)
Rank in Ordered Dataset
Enrichment profile
Hits
Ranking metric scores
B
HOS
β-catenin
Cyclin D1
c-myc
β-actin
85 kDa
36 kDa
45 kDa
42 kDa
Blank
si-NC
si-circ_001350-1
si-circ_001350-2
Relative protein expression
MG-63
C
HOS
LiCl
si-circ_001350-1 + LiCl
si-circ_001350-1+LiCl
D
HOS
si-NC + ov-NC
si-circ_001350-1 + ov-NC
si-NC + ov-CNOT7
si-circ_001350-1 + ov-CNOT7
si-NC+ov-NC
si-circ-1+ov-NC
si-NC+ov-CNOT7
si-circ-1+ov-CNOT7

Figure 7. Hsa_circ_001350 contributes to the proliferation, migration, and invasion of OS cells by regulating CNOT7/Wnt signaling. A. The CNOT7 elevation enriched Wnt signaling was analyzed by Gene Set Enrichment Analysis. B. HOS and MG-63 cells were transfected with hsa_circ_001350 siRNA-1 or hsa_circ_001350 siRNA-2. The protein expression of β-catenin, cyclin D1, and c-myc was measured by western blotting, followed by the quantification analysis using ImageJ. C. The protein expression of β-catenin, cyclin D1, and c-myc was measured by western blotting in HOS cells treated with 20 mM LiCl, hsa_circ_001350 siRNA-1 and the corresponding controls. D. The HOS cells were transfected with hsa_circ_001350 siRNA-1, or con-treated with hsa_circ_001350 siRNA-1 and pcDNA3.1-CNOT7. The protein expression of β-catenin, cyclin D1, and c-myc was assessed by western blotting in the cells, followed by the quantification analysis using ImageJ. N = 3, mean ± SD, $^{*}P < 0.05$ vs. si-NC or si-NC+ov-NC group, $^{\#}P < 0.05$ vs. si-circ_001350-1 or si-circ-1+ov-NC group, $^{\&}P < 0.05$ vs. LiCl or si-NC+ov-CNOT7 group.

These data elucidate a critical mechanism involving hsa_circ_001350 and miR-578 as modulators of OS progression.

CNOT7 is a key cytoplasmic mRNA deadenylase in metazoans [22]. In the study of cancer, CNOT7 exerts a carcinogenic effect on ovarian cancer via the AKT signaling pathway [23]. CNOT7 depletion reverses natural killer cell resistance by modulating the tumor immune microenvironment of hepatocellular carcinoma [14]. Moreover, CNOT7 is targeted by miR-126-5p and promotes breast cancer progression [13]. Our data showed that miR-578 targeted CNOT7 in OS cells.

Wnt signaling plays an essential role in OS development [24]. β-catenin is a key regulator of the Wnt/β-catenin pathway [25]. β-catenin accumulation promotes the transcription of downstream target genes and enhances the proliferation and metastasis of a tumor [26]. c-Myc is a downstream effector of β-catenin [27]. Studies have reported that c-Myc overexpression promotes OS cell invasion [28, 29]. CyclinD1 regulates cell proliferation by arresting cell cycle, whereas cyclinD1 inhibition expression relieves tumorigenicity [30]. Wang et al. have suggested that circ_0051079 silencing inhibits the malignant phenotype of OS cells via the miR-625-5p/TRIM66/Wnt/β-catenin pathway [31]. In addition, we found that hsa_circ_001350 depletion reduced the expression of β-catenin, c-myc and cyclinD1, which was reversed by CNOT7 overexpression. Our data showed that hsa_circ_001350 enhanced the malignant phenotype of OS cells by dysregulating CNOT7/Wnt signaling. These data revealed a novel correlation between hsa_circ_001350 and miR-578/CNOT7/Wnt signaling, showing a new regulatory network involved in OS pathogenesis.

Conclusions

In conclusion, we found that hsa_circ_001350 contributed to OS progression by dysregulating miR-578/CNOT7/Wnt signaling. Hsa_circ_001350, miR-578, and CNOT7 may be potential targets for the treatment of OS.

Acknowledgements

This study was supported in part by Hangzhou Medical Health Science and Technology Project. Project number: B20210313.

Disclosure of conflict of interest

None.

Address correspondence to: Xingyuan Ci, Laboratory Department, Hangzhou Linping First People's Hospital, No. 369, Yingbin Road, Linping District, Hangzhou 311400, Zhejiang, P. R. China. E-mail: cyyxy55@tom.com

References

[1] Kansara M, Teng MW, Smyth MJ and Thomas DM. Translational biology of osteosarcoma. Nat Rev Cancer 2014; 14: 722-735.

[2] Ritter J and Bielack SS. Osteosarcoma. Ann Oncol 2010; 21 Suppl 7: vii320-325.

[3] Marec-Berard P, Dalban C, Gaspar N, Brugieres L, Gentet JC, Lervat C, Corradini N, Castex MP, Schmitt C, Pacquement H, Tabone MD, Brahmi M, Metzger S, Blay JY and Perol D; OSII Thiotepa study group of the French Society of Pediatric Cancer - La Société Française des Cancers de l'Enfant (SFCE) and the French Sarcoma Group-Groupe d'Etude des Tumeurs Osseuses (GSF-GETO) Networks. A multicentric randomized phase II clinical trial evaluating high-dose thiotepa as adjuvant treatment to standard chemotherapy in patients with resectable relapsed osteosarcoma. Eur J Cancer 2020; 125: 58-68.

[4] Zils K, Bielack S, Wilhelm M, Werner M, Schwarz R, Windhager R, Hofmann-Wackersreuther G, Andus T, Kager L, Kuehne T, Reichardt P and von Kalle T. Osteosarcoma of the mobile spine. Ann Oncol 2013; 24: 2190-2195.
[5] Sun K, Gong C, Peng H, Fang H, Zhou J, Li J, Chen S and Zheng H. High CCL5 expression is associated with osteosarcoma metastasis and poor prognosis of patients with osteosarcoma. Mol Med Rep 2017; 16: 6953-6957.
[6] Chaichian S, Shafabakhsh R, Mirhashemi SM, Moazzami B and Asemi Z. Circular RNAs: a novel biomarker for cervical cancer. J Cell Physiol 2020; 235: 718-724.
[7] Kristensen LS, Andersen MS, Stagsted LVW, Ebbesen KK, Hansen TB and Kjems J. The biogenesis, biology and characterization of circular RNAs. Nat Rev Genet 2019; 20: 675-691.
[8] Liu Y, Ma C, Qin X, Yu H, Shen L and Jin H. Circular RNA circ_001350 regulates glioma cell proliferation, apoptosis, and metastatic properties by acting as a miRNA sponge. J Cell Biochem 2019; 120: 15280-15287.
[9] Xu L, Duan J, Li M, Zhou C and Wang Q. Circ_0000253 promotes the progression of osteosarcoma via the miR-1236-3p/SP1 axis. J Pharm Pharmacol 2023; 75: 227-235.
[10] Fan B, Chen F, Li Y, Wang Z, Wang Z, Lu Y, Wu Z, Jian J and Wang B. A comprehensive profile of the tilapia (Oreochromis niloticus) circular RNA and circRNA-miRNA network in the pathogenesis of meningoencephalitis of teleosts. Mol Omics 2019; 15: 233-246.
[11] Han B, Chao J and Yao H. Circular RNA and its mechanisms in disease: from the bench to the clinic. Pharmacol Ther 2018; 187: 31-44.
[12] Ji X, Shan L, Shen P and He M. Circular RNA circ_001621 promotes osteosarcoma cells proliferation and migration by sponging miR-578 and regulating VEGF expression. Cell Death Dis 2020; 11: 18.
[13] Miao Y, Lu J, Fan B and Sun L. MicroRNA-126-5p inhibits the migration of breast cancer cells by directly targeting CNOT7. Technol Cancer Res Treat 2020; 19: 1533033820977545.
[14] Ren C, Ren X, Cao D, Zhao H, Zhai Z, Li H, Li Y, Fu X, He J and Zhao H. CNOT7 depletion reverses natural killer cell resistance by modulating the tumor immune microenvironment of hepatocellular carcinoma. FEBS Open Bio 2020; 10: 847-860.
[15] Pridgeon MG, Grohar PJ, Steensma MR and Williams BO. Wnt signaling in ewing sarcoma, osteosarcoma, and malignant peripheral nerve sheath tumors. Curr Osteoporos Rep 2017; 15: 239-246.
[16] Zhang H, Yan J, Lang X and Zhuang Y. Expression of circ_001569 is upregulated in osteosarcoma and promotes cell proliferation and cisplatin resistance by activating the Wnt/β-catenin signaling pathway. Oncol Lett 2018; 16: 5856-5862.
[17] Cao J and Liu XS. Circular RNA 0060428 sponges miR-375 to promote osteosarcoma cell proliferation by upregulating the expression of RPBJ. Gene 2020; 740: 144520.
[18] Wang Z, Deng M, Chen L, Wang W, Liu G, Liu D, Han Z and Zhou Y. Circular RNA Circ-03955 promotes epithelial-mesenchymal transition in osteosarcoma by regulating miR-3662/metadherin pathway. Front Oncol 2020; 10: 545460.
[19] Sun L, Chen S, Wang T and Bi S. Hsa_circ_0008673 promotes breast cancer progression by MiR-578/GINS4 axis. Clin Breast Cancer 2022; 23: 281-290.
[20] Zhu S, Chen Y, Ye H, Wang B, Lan X, Wang H, Ding S and He X. Circ-LARP1B knockdown restrains the tumorigenicity and enhances radiosensitivity by regulating miR-578/IGF1R axis in hepatocellular carcinoma. Ann Hepatol 2022; 27: 100678.
[21] Hu R, Chen S and Yan J. Blocking circ-CNST suppresses malignant behaviors of osteosarcoma cells and inhibits glycolysis through circ-CNST-miR-578-LDHA/PDK1 ceRNA networks. J Orthop Surg Res 2021; 16: 300.
[22] Shirai YT, Suzuki T, Morita M, Takahashi A and Yamamoto T. Multifunctional roles of the mammalian CCR4-NOT complex in physiological phenomena. Front Genet 2014; 5: 286.
[23] Yu J, Hu X, Chen X, Zhou Q, Jiang Q, Shi Z and Zhu H. CNOT7 modulates biological functions of ovarian cancer cells via AKT signaling pathway. Life Sci 2021; 268: 118996.
[24] Singla A, Wang J, Yang R, Geller DS, Loeb DM and Hoang BH. Wnt signaling in osteosarcoma. Adv Exp Med Biol 2020; 1258: 125-139.
[25] Yu F, Yu C, Li F, Zuo Y, Wang Y, Yao L, Wu C, Wang C and Ye L. Wnt/β-catenin signaling in cancers and targeted therapies. Signal Transduct Target Ther 2021; 6: 307.
[26] Liu J, Xiao Q, Xiao J, Niu C, Li Y, Zhang X, Zhou Z, Shu G and Yin G. Wnt/β-catenin signalling: function, biological mechanisms, and therapeutic opportunities. Signal Transduct Target Ther 2022; 7: 3.
[27] Ren L, Zhou T, Wang Y, Wu Y, Xu H, Liu J, Dong X, Yi F, Guo Q, Wang Z, Li X, Bai N, Guo W, Guo M, Jiang B, Wu X, Feng Y, Song X, Zhang S, Zhao Y, Cao L, Han S and Xing C. RNF8 induces β-catenin-mediated c-Myc expression and promotes colon cancer proliferation. Int J Biol Sci 2020; 16: 2051-2062.
[28] Han G, Wang Y and Bi W. C-Myc overexpression promotes osteosarcoma cell invasion via activation of MEK-ERK pathway. Oncol Res 2012; 20: 149-156.

[29] Shin MH, He Y, Marrogi E, Piperdi S, Ren L, Khanna C, Gorlick R, Liu C and Huang J. A RUNX2-mediated epigenetic regulation of the survival of p53 defective cancer cells. PLoS Genet 2016; 12: e1005884.
[30] Tashiro E, Tsuchiya A and Imoto M. Functions of cyclin D1 as an oncogene and regulation of cyclin D1 expression. Cancer Sci 2007; 98: 629-635.
[31] Li S, Lei Z, Yang X, Zhao M, Hou Y, Wang D, Tang S, Li J and Yu J. Propofol protects myocardium from ischemia/reperfusion injury by inhibiting ferroptosis through the AKT/p53 signaling pathway. Front Pharmacol 2022; 13: 841410.